Cell Transplantation
2019, Vol. 28(12) 1674–1685

DOI: 10.1177/0963689719874048
journals.sagepub.com/home/cll
SAGE

Endothelial Progenitor Cells Attenuate Ventilator-Induced Lung Injury with Large-Volume Ventilation

Ying-nan Ju[1], Ying-jie Geng[2], Xue-ting Wang[2], Jing Gong[2], Jingli Zhu[2], and Wei Gao[2]

Abstract

Ventilator-induced lung injury (VILI) is a common complication that results from treatment with mechanical ventilation (MV) in acute respiratory distress syndrome (ARDS) patients. The present study investigated the effect of endothelial progenitor cell (EPC) transplantation on VILI. Wistar rats were divided into three groups ($n = 8$): sham (S), VILI model (V) induced by tidal volume ventilation (17 mL/kg), and VILI plus EPC transplantation (VE) groups. The lung PaO_2/FiO_2 ratio, pulmonary wet-to-dry (W/D) weight ratio, number of neutrophils, total protein, neutrophil elastase level, and inflammatory cytokines in bronchoalveolar lavage fluid (BALF) and serum were examined. Furthermore, the histological and apoptotic analysis, and lung tissue protein expression analysis of Bax, Bcl-2, cleaved caspase-3, matrix metalloproteinase (MMP)-9, total nuclear factor kappa B (total-NF-κB), phosphorylated NF-κB (phospho-NF-κB) and myosin light chain (MLC) were performed. The ventilation-induced decrease in PaO_2/FiO_2 ratio, and the increase in W/D ratio and total protein concentration were prevented by the EPC transplantation. The EPC transplantation (VE group) significantly attenuated the VILI-induced increased expression of tumor necrosis factor (TNF)-α, interleukin (IL)-1β, IL-8, MMP-9, phospho-NF-κB and MLC, neutrophil elastase levels and neutrophil counts in BALF. In addition, the anti-inflammatory factor IL-10 increased in the VE group. Furthermore, pulmonary histological injury and apoptosis (TUNEL-positive cells, increase in Bax and cleaved caspase-3) were considerably diminished by the EPC transplantation. The EPC transplantation ameliorated the VILI. The mechanism may be primarily through the improvement of epithelial permeability, inhibition of local and systemic inflammation, and reduction in apoptosis.

Keywords

endothelial progenitor cell, ventilator, acute lung injury, mechanical ventilation

Introduction

Mechanical ventilation (MV) is essential for respiratory support and treating patients with pulmonary dysfunction. It has been reported that approximately 39% of patients need MV support in intensive care units[1]. Patients with acute respiratory distress syndrome (ARDS) experience ventilator-induced lung injury (VILI)[2], which has a 40% mortality rate[3]. Although volutrauma, pressuretrauma, and atelectrauma contribute to VILI, the excess pressure within the alveoli is the initial cause of VILI. During the process of MV, gas flows into the lungs through the path of least resistance. Thus, collapsed (at electasis) areas or secretion-filled spaces would be underinflated, and the remaining areas would be overinflated and distended, leading to injury[4]. In addition, repetitive cyclic stretch, regional lung deformation, and/or overinflation of the alveoli induced by large tidal volume ventilation could directly injure the endothelium and epithelium, and further increase alveolar–capillary permeability, leading to lung edema[5] and inflammatory disorders[4]. Although certain measures have been suggested to ameliorate lung injury[3], even a small tidal volume MV could result in VILI[6,7]. The mortality of ARDS patients remains at

[1] Department of Intensive Care Unit, The Third Affiliated Hospital of Harbin Medical University, Harbin, Heilongjiang Province, China
[2] Department of Anesthesiology, The Second Affiliated Hospital of Harbin Medical University, Harbin, Heilongjiang Province, China

Submitted: March 23, 2019. Revised: August 6, 2019. Accepted: August 13, 2019.

Corresponding Author:
Wei Gao, Department of Anesthesiology, The Second Affiliated Hospital of Harbin Medical University, 246 Xuefu Road, Harbin 150081, Heilongjiang Province, China.
Email: gaowei20055@126.com

approximately 25–45%[8]. Even though noninvasive ventilation is extensively applied in ARDS patients, hospital mortality remains within 16.1–45.4%[9].

The mechanistic details of VILI remain unclear. Nevertheless, the main pathology of VILI has been considered to be caused by the imbalance in pro- and anti-inflammatory cytokines[10,11]. Following the stimulation by air pressure forces during MV, mechanically injured endothelial and epithelial cells evoke focal inflammatory responses[12], and release inflammatory cytokines that infiltrate the lung tissue. Under the action of pro-inflammatory factors, alveolar–capillary permeability increases, which directly results in lung edema[13].

Endothelial progenitor cells (EPCs) have been reported to have a therapeutic effect during acute lung injury and myocardial ischemia[14] as a result of their regenerative and anti-inflammatory properties. The transplantation of EPCs has been shown to improve endothelial function and preserve the integrity of the alveolar–capillary barrier, thereby increasing the survival rate of rats with acute lung injury[15]. The protective effect of EPC transplantation on pulmonary organ injury is not only due to the vascular regeneration or repair of the endothelial lining, but also attributed to the regulation of the immune system[16].

Considering the pivotal pathological role of inflammation in VILI and the EPC-mediated regulation of the immune system, the investigators hypothesized that EPC transplantation could attenuate the VILI caused by large-volume ventilation. In the present study, rat EPCs were transplanted to rat a VILI model to explore its therapeutic effect on rat lung injury. The present study may provide evidence for additional VILI clinical treatment options, especially in ventilatory therapy, for patients with preinjured lungs or pulmonary dysfunction.

Materials and Methods

Isolation and Culture of EPCs

The present study was approved by the Ethics Committee of Harbin Medical University. All treatments were performed according to the Institutional Animal Care and Use Committee of the Second Affiliated Hospital of Harbin Medical University and national animal treatment guidelines.

Peripheral blood was withdrawn from the caudal vein of Wistar rats (6–8 weeks, 140–160 g), and mononuclear cell isolation was achieved using density gradient centrifugation with Ficoll-Plaque Plus (Amersham Pharmacia Biotech AB, Uppsala, Sweden). After washing with phosphate-buffered saline (PBS), the isolated mononuclear cells were incubated in complete endothelial growth medium (EGM)-2 (Lonza Corp., Basel, Switzerland) on six-well plates pre-coated with human fibronectin at 37°C with 5% CO_2. The culture medium was changed daily. After 10 days of culture, the EPCs were lifted with 0.025% trypsin containing 0.02% EDTA and harvested for further analysis or transplantation.

Characterization of EPCs

The EPCs isolated from rats were identified using a methodology from a previous study[17,18]. Mononuclear cells were incubated with Dil-acetyl-low density lipoprotein (LDL, 10 μg/mL; Invitrogen, Carlsbad, CA, USA) and fluorescein isothiocyanate-ulexeuropaeus agglutinin-1 (UEA-1, 5 μg/mL; Sigma-Aldrich, Saint Louis, MO, USA). EPCs stained with DiI-acetyl-LDL (absorption wavelength: 555 nm) and UEA-1 (absorption wavelength: 495 nm) were identified using a confocal microscope. These EPCs were also stained with vascular endothelial growth factor receptor (VEGFR)-2 (Abcam, Cambridge, UK), CD34, and CD133 (Santa Cruz Biotechnology, Santa Cruz, California, USA), as described in a previous study[17,19]. Furthermore, in order to characterize the subtype of EPCs, cells with antibodies against FITC-CD14 (Santa Cruz Biotechnology) and PE-CD45 (Biolegend, San Diego, CA, USA) were analyzed using a flow cytometer. $CD14^-/CD45^-$ cells were considered as advanced EPCs (endothelial colony-forming cells), while $CD14^+/CD45^+$ cells were considered as early EPCs[20].

VILI Model and EPC Transplantation

All male Wistar rats (250–280 g) were fed with water and standard diet *ad libitum* before the study. Twenty-four rats were randomly divided into three groups ($n = 8$/group): sham group (S group), ventilation group (V group), and ventilation/EPC transplantation group (VE group). Rats in the S group were only exposed to anesthesia, while rats in the V and VE groups received MV, with a tidal volume of[21] 17 mL/kg (inspiratory gas: 50% O_2 + 50% N_2; 50% respiratory rate: 50/min; inspiratory to expiratory ratio: 1:1) for 4 h. Then, all rats were anesthetized with 3% pentobarbital sodium (a total volume of 30 mg/kg) via intraperitoneal (IP) injection. Following local analgesia with lidocaine, peripheral blood was collected through cannulation of the caudal vein and artery for arterial blood gas analysis. In addition, saline infusion was achieved through cannulation. After additional anesthesia with a rocuronium injection (0.6 mg/kg), rats in the V and VE groups were intubated with a 14 G tube and exposed to MV (a tidal volume of 17 mL/kg for 4 h). Rats in the VE group were intravenously given approximately 10^6 of EPCs (in 1 mL of PBS) immediately at the end of MV[22]. PBS alone was intravenously given to rats in the V group as controls. The anesthesia was maintained with 3% pentobarbital sodium (10 mg/kg) and rocuronium (0.6 mg/kg) over 1-h intervals. Once spontaneous breath recovered after 4 h of ventilation, the rats were extubated. All rats were anesthetized and cannulated. After the collection of blood samples, all rats were sacrificed with an overdose of anesthetics at 24 h following ventilation[23].

Arterial Blood Gas Analysis

In order to observe the effect of EPC transplantation on pulmonary gas exchange function, arterial blood gases were

analyzed at baseline and at 24 h after ventilation using a Bayer Rapid lab 348 ventilator (Bayer Diagnostics, Leverkusen, Germany). The ratio of oxygen partial pressure to fraction inspiratory oxygen (PaO_2/FiO_2) was calculated.

Alveolar–Capillary Permeability

After sacrifice at 24 h after ventilation, the right upper lung lobes of rats were harvested and weighed while wet. Then, these were dried at 60°C for 48 h and weighed again. Afterwards, the wet/dry weight (W/D) ratio was calculated to indirectly determine the effect of the EPC transplantation on alveolar–capillary permeability[24,25].

Inflammatory Cytokine Detection in Bronchoalveolar Lavage Fluid and Serum

The right bronchus was blocked using an artery clamp. Then, sterile saline (4°C, 15 mL/kg) was injected into the left lung and withdrawn from the pulmonary airway for five times. Next, bronchoalveolar lavage fluid (BALF) was collected and centrifuged (1,000 × *g*, 15 min, 4°C). The cytokines in the supernatant of the BALF, including interleukin (IL)-1β, IL-8, IL-10, tumor necrosis factor (TNF)-α, and neutrophil elastase, were detected using the corresponding ELISA kit (Wuhan Boster Bio-Engineering Limited Company, Wuhan, China), according to product instructions. The protein concentration in the supernatant of the BALF and neutrophil count in the BALF pellet were also measured.

Peripheral femoral venous blood was collected at baseline and at 24 h after ventilation, and centrifuged (1,500 × *g*, 4°C, 10 min). Then, the serum (supernatant) was transferred into a separate Eppendorf tube and stored at –80°C. The levels of IL-1β, IL-8, IL-10, TNF-α, macrophage inflammatory protein (MIP)-2, and intercellular adhesion molecule (ICAM)-1 were detected using the corresponding ELISA kits above.

Histopathologic Injury Examination

The lung tissue harvested from the lower right lobe was used to examine the histological alterations. The tissue was fixed with 4% paraformaldehyde, embedded in paraffin, cut in 4-μm-thick sections, and placed onto a glass slide. Then, the treated lung tissue on the slide was stained with hematoxylin and eosin (H&E). Two blinded independent pathologists evaluated the extent of lung injury under a light microscope. The pathological alterations that were analyzed included edema, alveolar congestion, hemorrhage, airspace/vessel wall neutrophil infiltration, alveolar wall thickness, and hyaline membrane formation. The histological score was evaluated from 0 to 4 (0, normal histological presentation; 1, light infiltration of inflammatory cells; 2, severe perivascular infiltration of inflammatory cells; 3, infiltration of inflammatory cells in the alveolar septum/space; 4, diffused infiltration of mononuclear cells in the perivascular, interstitial and airspace).

Tracking of Transplanted EPCs in Lung Tissue

In order to identify the distribution of EPCs in lung tissue and distinguish the EPCs injected from EPCs derived from rats, EPCs with acetyl-LDL (37°C for 2 h) were pre-labeled and injected into another eight rats. Then, the transplanted acetyl-LDL-labeled EPCs were detected in rat pulmonary tissue using a fluorescent microscope. Briefly, after 24 h, the harvested pulmonary tissue was fixed with paraformaldehyde and embedded in paraffin. The sectioned pulmonary tissue on a glass slide was deparaffinized with xylene and rehydrated with decreasing alcohol gradients. The slide was stained with 4,6-diamidino-2-phenylindole (DAPI; 1 μg/mL) for 30 min to visualize the nuclei. The distribution of EPCs in lung tissue was finally detected using a confocal microscope (absorption wavelength: 555 nm for acetyl-LDL).

Apoptosis Assay

Pulmonary tissues from the right middle lobe was collected to detect the apoptosis by TUNEL staining using an apoptosis assay kit (Roche, Mannheim, Germany). Briefly, the sectioned pulmonary tissue on a slide was immersed with proteinase K at 37°C for 30 min. After washing with PBS twice, the slide was immersed in the TUNEL reaction mixture (TdT and fluorochrome-conjugated dUTP) at 37°C for 60 min in a dark chamber, incubated with DAPI (1 μg/mL) for 30 min, and visualized using a confocal microscope (absorption wavelength: 490 nm).

Western Blot

Protein was extracted from the right lung, and the protein concentration was determined using the Bradford assay. Aliquot amounts of the protein for each sample were loaded onto a SDS-polyacrylamide gel, and transferred onto a polyvinylidene fluoride (PVDF) membrane. Then, the membrane was blocked with 5% milk for 30 min, and incubated with a primary antibody overnight at 4°C. The primary antibodies included the following: Bax, Bcl-2, matrix metalloproteinase (MMP)-9, cleaved caspase-3 (Sigma-Aldrich), phosphorylated myosin light chain (phospho-MLC; Sigma-Aldrich), and total nuclear factor kappa B (total-NF-κB) and phosphorylated NF-κB (phospho-NF-κB) (Santa Cruz Biotechnology). After washing with TBS-tween buffer (3 × 5 min), the membrane was incubated with horseradish peroxidase (HRP)-linked secondary antibodies (Santa Cruz Biotechnology) for 1 h, and the probed-bands on the membrane were visualized by enhanced chemiluminescence.

Statistical Analysis

Normally distributed data were presented as mean ± standard deviation (SD), and statistically analyzed by repeated

measures analysis of variance (ANOVA) (with Bonferroni post-hoc test) using the SPSS 11.0 software (SPSS, Chicago, IL, USA). $p < 0.05$ was considered statistically significant.

Results

Characterization of EPCs

Rat peripheral blood mononuclear cells were isolated by density gradient centrifugation. After 10 days of incubation, approximately $8–10\times10^6$ cells proliferated, and were analyzed. Endothelial cells expressed DiI-acetyl-LDL (Fig. 1A) and isothiocyanate-UEA-1 (Fig. 1B). The merged image of the anti-UEA-1 and DiI-ac-LDL staining is presented in Fig. 1C. The expression of both (Figs 1C) was detected using fluorescent antibodies in the isolated monolayer of cells. These results demonstrate that the monolayer of cells were endothelial cells. The biological characteristics of EPCs were further identified by the positive staining of VEGFR-2 (Fig. 1D) and CD34 (Fig. 1E). The merged image of the anti-VEGFR-2 and CD34 staining is presented in Fig. 1F. VEGFR-2 (Fig. 1G) and CD133 (Fig. 1H) were also detected. The merged image of the VEGFR-2 and CD133 staining is presented in Fig. 1I. These data indicate that the isolated monolayer of cells were EPCs. Furthermore, all analyzed EPCs presented as spindle-shaped (Fig. 1J). The subtype of EPCs was also characterized with FITC-CD14 and PE-CD45 using a flow cytometer. The percentage of $CD14^+/CD45^+$ cells was 14.6 ± 3.2, while the percentage of $CD14^-/CD45^-$ cells was 40.5 ± 4.1 (Fig. 1K and 1L). Furthermore, some cells were also found with $CD14^+/CD45^-$ and $CD14^-/CD45^+$. At present, no study has named or classified these cells. Hence, it was hypothesized that these cells may be special cells between early and advanced EPCs. However, this hypothesis needs further studies to be confirmed.

Detection of Transplanted EPCs

The EPCs transplanted in rat lungs in the VE group were observed by immunofluorescent staining using an acetyl-LDL (Fig. 2A) antibody and DAPI (Fig. 2B) with fluorescence microscopy. It was found that these EPCs were successfully transplanted and survived in rat lungs in the VE group (Fig. 2C). In contrast, samples obtained from rats in the V group did not show any acetyl-LDL staining (Fig. 2D).

EPCs Improved the Gas Exchange Index and Alveolar–Capillary Permeability

In the present study, the PaO_2/FiO_2 index significantly decreased at post-ventilation 24 h in the V and VE groups, when compared with the S group ($p < 0.05$). The EPC transplantation (VE group) dramatically increased the PaO_2/FiO_2 ratio, when compared with the V group (Fig. 3A, $p < 0.05$). In addition, the pulmonary W/D weight ratio and total protein in the BALF were analyzed to detect the effect of EPCs on alveolar–capillary permeability. Interestingly, the pulmonary W/D weight ratio (Fig. 3B) and total protein level in the BALF (Fig. 3C) were significantly higher in the V and VE groups, when compared with the S group ($p < 0.05$). However, this increase significantly declined after EPC transplantation (VE group, $p < 0.05$). These results clearly demonstrate that the transplantation of EPCs significantly attenuated the VILI in the rat model.

Local and Systemic Inhibition of Inflammation by Transplanted EPCs

The concentration of various inflammatory cytokines, including TNF-α (Fig. 3D), IL-1β (Fig. 3E), IL-8 (Fig. 3F), and IL-10 (Fig. 3G), as well as the neutrophil count (Fig. 3H) and neutrophil elastase (Fig. 3I), in the BALF was measured to explore the effect of EPCs on local inflammation in the rat VILI model. The levels of TNF-α, IL-1β, IL-8, and neutrophil elastase, and neutrophil count in the BALF were significantly higher in the V and VE groups, when compared with the S group ($p < 0.05$). However, these elevations significantly decreased after the EPC transplantation (VE group, $p < 0.05$). In contrast, the level of IL-10 was significantly upregulated by the EPC transplantation (VE group), when compared with the V group ($p < 0.05$).

Next, the serum levels of TNF-α (Fig. 3J), IL-1β (Fig. 3K), IL-8 (Fig. 3L), IL-10 (Fig. 3M), ICAM-1 (Fig. 3N), and MIP-2 (Fig. 3O) were analyzed to explore the effect of EPCs on systemic inflammation in the rat VILI model. All cytokines in serum were upregulated by ventilation (V and VE groups), when compared with the S group ($p < 0.05$). Similar to the responses in the BALF, the levels of TNF-α, IL-1β, IL-8, ICAM-1, and MIP-2 significantly decreased after EPC transplantation (VE group), when compared with the V group ($p < 0.05$). However, the level of IL-10 was significantly upregulated after the EPC transplantation (VE group, $p < 0.05$; Fig. 3M).

Compared with the S group, MMP-9, total-NF-κB, phospho-NF-κB, and phospho-MLC were significantly upregulated following ventilation (V and VE groups, $p < 0.05$). However, these upregulations were considerably attenuated by the lung transplantation of EPCs (VE group), when compared with the V group (Fig. 4).

EPC Transplantation Attenuated Ventilation-Induced Histological Injury in the Rat VILI Model

The effect of EPC transplantation on histological changes in the rat VILI model was evaluated by H&E staining. Compared with the S group (Fig. 5A), typical pathological changes, including edema, alveolar wall thickening, the formation of a hyaline membrane, and hemorrhage, were observed in the V (Fig. 5B) and VE groups (Fig. 5C). However, these alterations were milder in the EPC transplantation (VE group) samples than those in the V group (Fig. 5D).

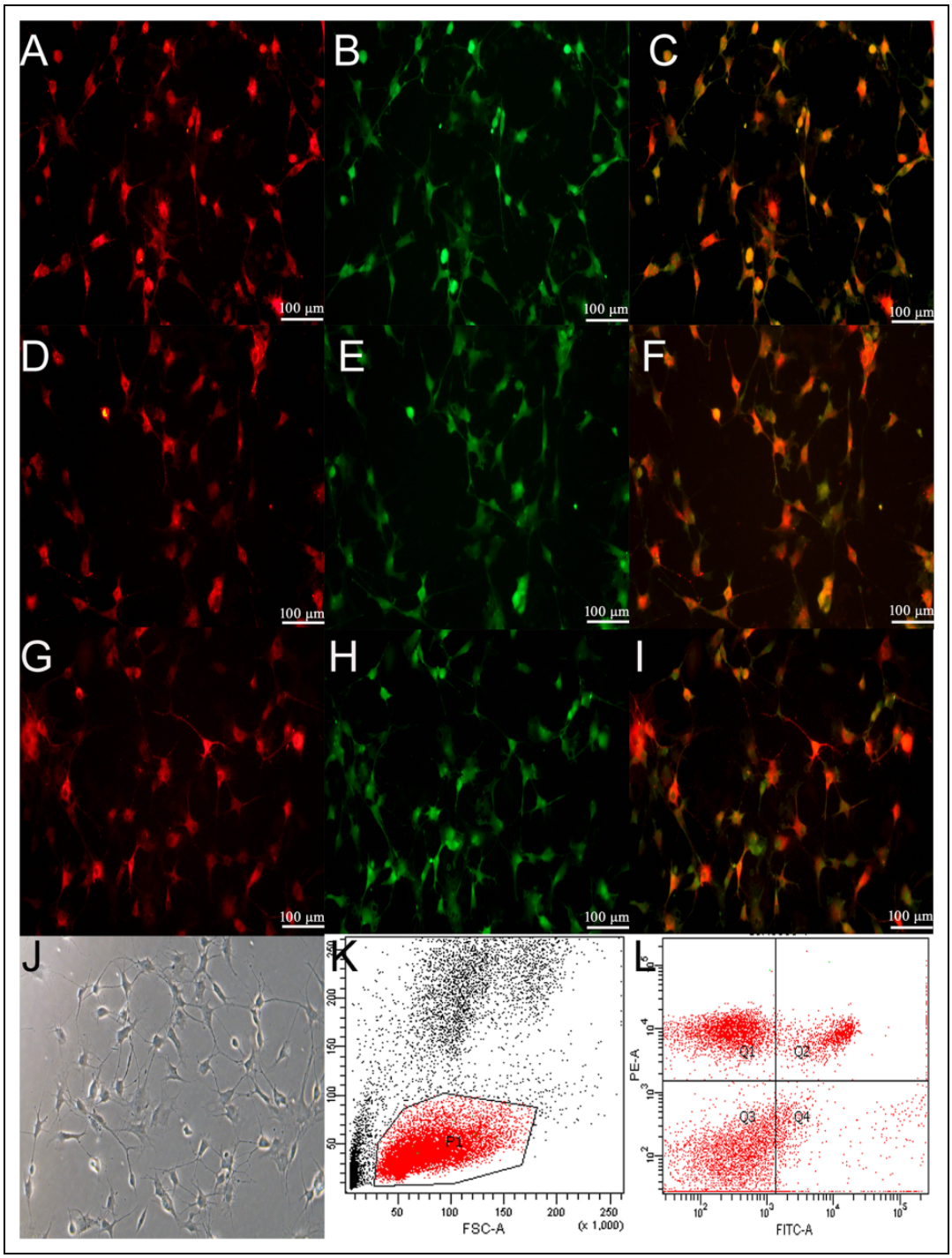

Figure 1. Characterization of EPCs. Rat peripheral blood mononuclear cells were isolated by density gradient centrifugation, as described in the Materials and Methods. The endothelial characteristics were identified through the positive staining of both DiI-acetyl-LDL (A, red) and FITC-UEA-1 (B, green). The merged image of DiI-acetyl-LDL and FITC-UEA-1 is presented in C (yellow). Furthermore, EPCs were recognized through the cytoplasmic positive signals of both VEGFR-2 (D, 400 × magnification, red) and CD34 (E, 400 × magnification, green). The merged image of VEGFR2 and CD34 is presented in F (yellow). In addition, EPCs were identified with VEGFR-2 (G, 400 × magnification, red) and CD133 (H, 400 × magnification, green). The merged image of VEGFR2 and CD34 is presented in I (yellow). From the tenth day after isolation, these cells were characteristic of a monolayer (J, 400 × magnification). Abbreviations: EPCs, endothelial progenitor cells; LDL, low density lipoprotein; UEA-1, ulexeuropaeus agglutinin-1; VEGFR2, vascular endothelial growth factor receptor 2.

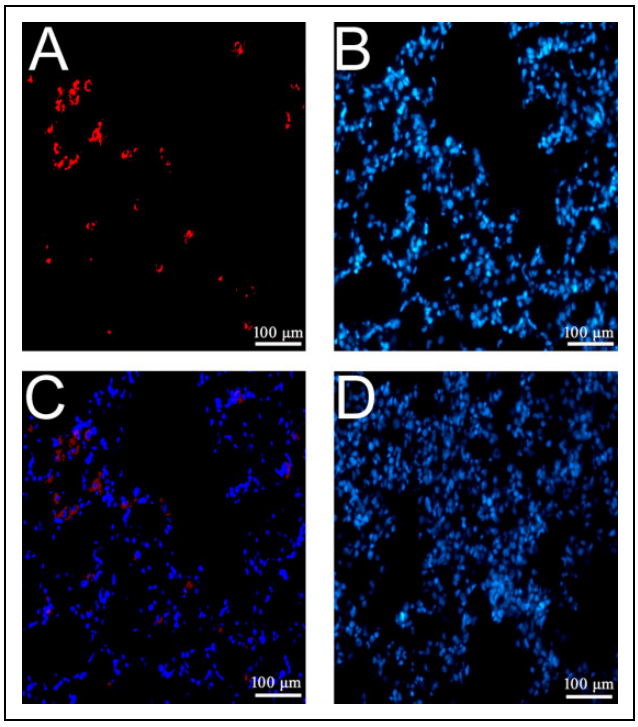

Figure 2. Tracking EPCs following the transplantation in lung tissue. EPCs transplanted to lung tissues at 24 h after injection were detected and identified by acetyl-LDL immunofluorescence staining. The positive acetyl-LDL stain presented as red (A), and the nuclei was visualized by DAPI (blue, B). The merged image is presented in C (200 × magnification). The DAPI stain in the tissue of rats in the V group is presented in D. Abbreviations: DAPI, 4-,6-diamidino-2-phenylindole; EPCs, endothelial progenitor cells; LDL, low density lipoprotein. Each testing group contained eight rats.

EPC Transplantation Reduced Ventilation-Induced Apoptosis in the Rat VILI Models

Compared with the S group (Fig. 6Aa), an increased number of TUNEL-positive cells (green) was observed in the V group (Fig. 6Ab). However, the EPC transplantation (Fig. 6Ac) reduced the number of TUNEL-positive cells in the VE group, when compared with the VILI model (V group). In addition, the expression of Bax (Fig. 6Ba and 6Bb) and both cleaved (Fig. 6Ba and 6Be) and uncleaved (Figs 6Ba and 6 Bd) caspase-3, which are critical factors to regulate the apoptotic process, was significantly higher in the V group, and this increase could be partially prevented by EPC transplantation (VE group). In contrast, the expression of Bcl-2 (Fig. 6Ba and 6Bc), which is a critical anti-apoptotic factor, significantly decreased in the rat VILI model (V group), and the decrease in Bcl-2 was partially attenuated by EPCs.

Discussion

In the present study, it was demonstrated that the EPC transplantation significantly ameliorated lung histological injury and apoptosis, improved alveolar–capillary permeability, and reduced inflammation, thereby reducing the effects caused by the VILI.

A previous study indicated that EPCs obviously reduced the lung injury induced by endotoxin and oleic acid. However, in the clinic, more VILI patients are associated with the lung injury induced by the ventilator, especially the long-term ventilation for major surgery. The statistical data revealed that approximately 39% of patients in the ICU need ventilation support[1]. Even a single ventilation with 40 cm H_2O could result in the release of biomarkers (type III procollagen)[26]. Furthermore, mechanical ventilation[27] leads to local and systemic inflammation in patients with normal pulmonary function. Therefore, the effect of EPCs on VILI induced by MV was evaluated in the present study.

The impairment of endothelial function is a pathological feature of VILI, which can cause pulmonary edema, surfactant dysfunction, and the deterioration of pulmonary gas exchange[21]. During VILI, the disruption of the pulmonary endothelial barrier is mainly caused by myosin light chain (MLC) phosphorylation[28]. In addition, Mirzapoiazova et al. validated MLC as an attractive target to ameliorate dysregulated lung inflammation[29]. The results of the present study suggest that EPC transplantation can significantly decrease the VILI-induced phosphorylation of MLC. Therefore, it was postulated that the effect of EPCs on the MLC may be one of the possible mechanisms of the EPC-mediated improvement of the VILI.

In addition to the effect of EPCs on the MLC, the anti-inflammatory effect of EPCs may contribute to lung protection. During the VILI, the activation and phosphorylation of NF-κB would trigger the activation of inflammatory cells and the formation of a chemoattractant gradient, which induces an inflammatory cascade[30,31]. These activated neutrophils are rich in MMP-9, and increase under pathological conditions[32], leading to local and systemic inflammation[33]. The reduction or inhibition of NF-κB and MMP-9 have been shown to improve ARDS and VILI[30,34]. VILI-induced pulmonary inflammation has been reported to be closely associated with MMP-9 and NF-κB, and the suppression of MMP-9 or TNF-α could protect against VILI-induced neutrophil-mediated inflammation[34,35]. These results were further confirmed in the rat VILI model, which demonstrates not only the increase in neutrophil infiltration, but also the upregulation of TNF-α, MMP-9 and other pro-inflammatory factors, including IL-1β, IL-8 and neutrophil elastase, in both the BALF and serum. Importantly, EPC transplantation attenuated these alterations. The present data also revealed that total-NF-κB and phospho-NF-κB were significantly reduced by the EPC transplantation, which is consistent with previous findings[36]. These studies indicate that EPCs may protect organ injury through the attenuation of the activation of NF-κB induced by the inflammation and oxidative stress response. These data also indicate that the anti-inflammation of EPCs may be mainly due to the inhibition of EPCs on NF-κB[22,36–38]. Interestingly, in contrast to pro-inflammatory factors, the EPC transplantation considerably upregulated

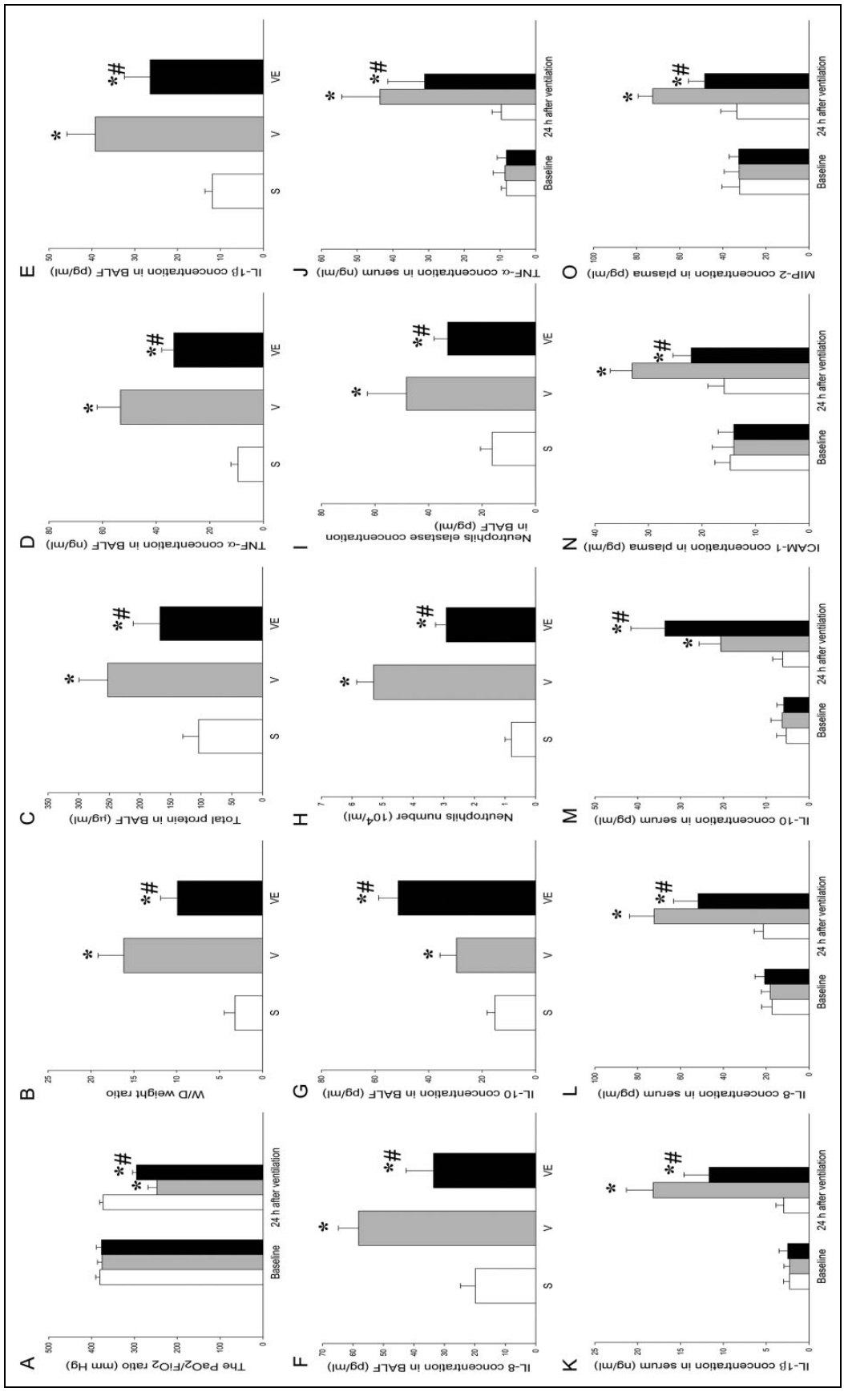

Figure 3. The lung transplantation of EPCs improved the ventilation-induced PaO_2/FiO_2 ratio, W/D weight ratio and protein concentration. The PaO_2/FiO_2 ratio (A), lung W/D weight ratio (B), and protein concentration in the BALF (C) were analyzed in the samples obtained from rats in the S group. The VILI model and EPC transplanted rats before (left) and after 24-h ventilation (right) are presented. Each testing group contained eight rats. $^{*}p < 0.05$ *vs.* the S group; $^{\#}p < 0.05$ *vs.* the V group. Abbreviations: BALF, bronchoalveolar lavage fluid; EPCs, endothelial progenitor cells; PaO_2/FiO_2, partial pressure of O_2 to fraction inspiratory O_2; S group, sham; VILI, ventilator-induced lung injury; W/D, pulmonary wet/dry weight. The levels of TNF-α (D), IL-1β (E), IL-8 (F), IL-10 (G), neutrophil count (H), and neutrophil elastase (I) in the BALF were examined in the S, V, and VE groups by ELISA assay. $^{*}p < 0.05$ *vs.* the S group; $^{\#}p < 0.05$ *vs.* the V group. The serum levels of TNF-α (J), IL-1β (K), and IL-8 (L), IL-10 (M), ICAM-1 (N) and MIP-2 (O) in the S group (□), V group (▒) and VE group (■) were detected using the corresponding ELISA kits before (left panels) and after (right panels) ventilation. $^{*}p < 0.05$, when compared with the S group; $^{\#}p < 0.05$, when compared with the V group. Abbreviations: ELISA, enzyme-linked immunosorbent assay; EPCs, endothelial progenitor cells; ICAM, intercellular adhesion molecule; IL, interleukin; MIP, macrophage inflammatory protein; S group, sham; TNF, tumor necrosis factor; V group, VILI group; VE group, VILI with EPC transplantation; VILI, ventilator-induced lung injury. Each testing group contained eight rats.

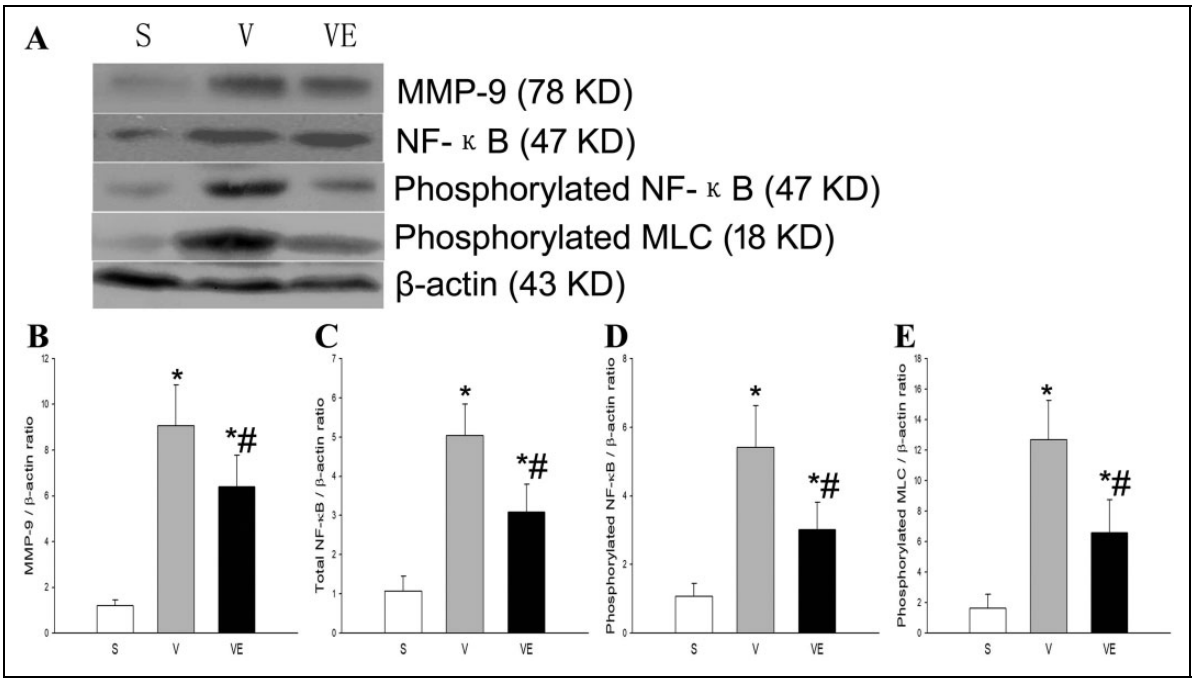

Figure 4. EPC transplantation decreased the ventilation-induced increase of MMP-9, phosphorylated NF-κB and phosphorylated MLC in the rat VILI model. The representative results of the expression of MMP-9 (upper panel of A and B), total-NF-κB (secondary panel of A and C), phosphorylated NF-κB (third panel of A and D), and phosphorylated MLC (forth panel of A and E) in lung tissues in the S group (left bands of A and □ of B–E), V group (middle bands of A and ▒ of B–E) and VE group (right bands of A and ■ of B–E) were detected by Western blot. The corresponding protein expression was evaluated by densitometry and presented in B (MMP-9), C (total-NF-κB), D (phosphorylated NF-κB), and E (phosphorylated MCL). Data from each group were calculated from three independent experiments. $^{*}p < 0.05$, when compared with the S group; $^{\#}p < 0.05$, when compared with the V group. Abbreviations: EPCs, endothelial progenitor cells; MLC, myosin light chain; MMP, matrix metalloprotease; NF-κB, nuclear factor kappa B; S group, sham; V group, VILI; VE group, VILI with EPC transplantation; VILI, ventilator-induced lung injury.

anti-inflammatory factor IL-10 in both the BALF and serum in the VE group. Similar results demonstrating the immune regulation properties of EPCs have been previously reported.

In VILI, an oxidative stress response and inflammatory response could activate the extrinsic and intrinsic apoptotic pathways[39,40]. In the present study, the apoptotic cells in pulmonary tissues were observed after ventilation (V group) and ventilation + EPC transplantation (VE group), and the results indicated that apoptosis was significantly reduced after the EPC transplantation[14]. In addition, Bax is an important pro-apoptotic protein, while Bcl-2 is an anti-apoptotic protein that can prevent the activation of Bax. An increase or decrease in apoptosis has been shown to primarily depend on the Bax-to-Bcl-2 ratio[41]. During VILI or ARDS, the increase in gelsolin was able to promote neutrophil infiltration and epithelial apoptosis[42–46]. Under pro-apoptotic signaling, caspase-3 is activated (cleaved) and cuts the DNA to mediate cellular apoptosis. In the present study, it was found that the EPC transplantation inhibited the VILI-induced apoptosis. The anti-apoptotic activity of EPCs appeared to be associated with the regulation of Bax, Bcl-2 and cleaved caspase-3, since the EPC transplantation significantly decreased the expression of Bax, full-length caspase-3, and cleaved caspase-3, and promoted the expression of Bcl-2.

Regarding the limitations of the present study, positive end-expiratory pressure was not applied as a control, since positive end-expiratory pressure is an effective therapy for VILI, which could have influenced the results of EPCs on the VILI. Furthermore, the peak, plateau pressure, and compliance were not monitored because of the lack of monitoring apparatus. Moreover, in the present study, although the EPCs used contained both early EPCs and advanced EPCs, these mainly contained advanced EPCs. It has been indicated that advanced EPCs directly participate in tubulogenesis, while early EPCs augment angiogenesis in a paracrine fashion, with implications for optimizing cell therapies for neovascularization[47]. In future studies, focus would be given in determining the exact mechanism of early or advanced EPCs on VILI using a cell culture model.

For the limitation of the present study, it was assumed that EPCs reduce the inflammation possibly via the inhibition of NF-κB in endothelial cells. However, NF-κB inhibitors and agonists were not administered to verify this hypothesis,

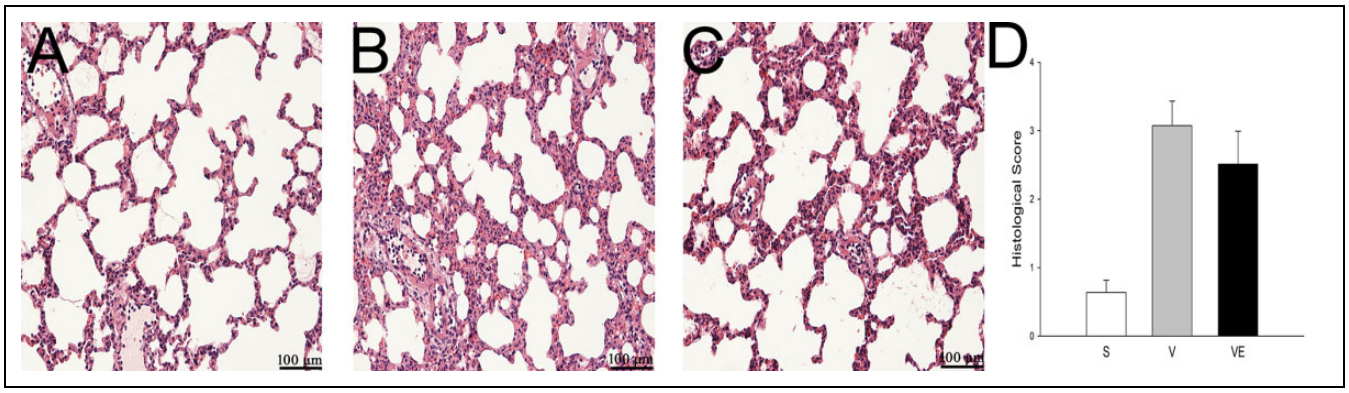

Figure 5. EPC transplantation attenuated histological lung injury in the rat VILI model. The histopathological alteration of lung tissue in the S (A and D), V (B and E), and VE (C and F) groups were analyzed by H&E staining. A-C: 200 × magnification; D-F: 400 × magnification. The histological change in the V group (B and E) revealed a thickened alveolar wall, pulmonary edema, broken alveoli and hemorrhage. EPC transplantation (VE group) clearly mitigated these alterations (C and E). Abbreviations: EPCs, endothelial progenitor cells; H&E, hematoxylin and eosin; S group, sham; V group, VILI; VE group, VILI with EPC transplantation; VILI, ventilator-induced lung injury.

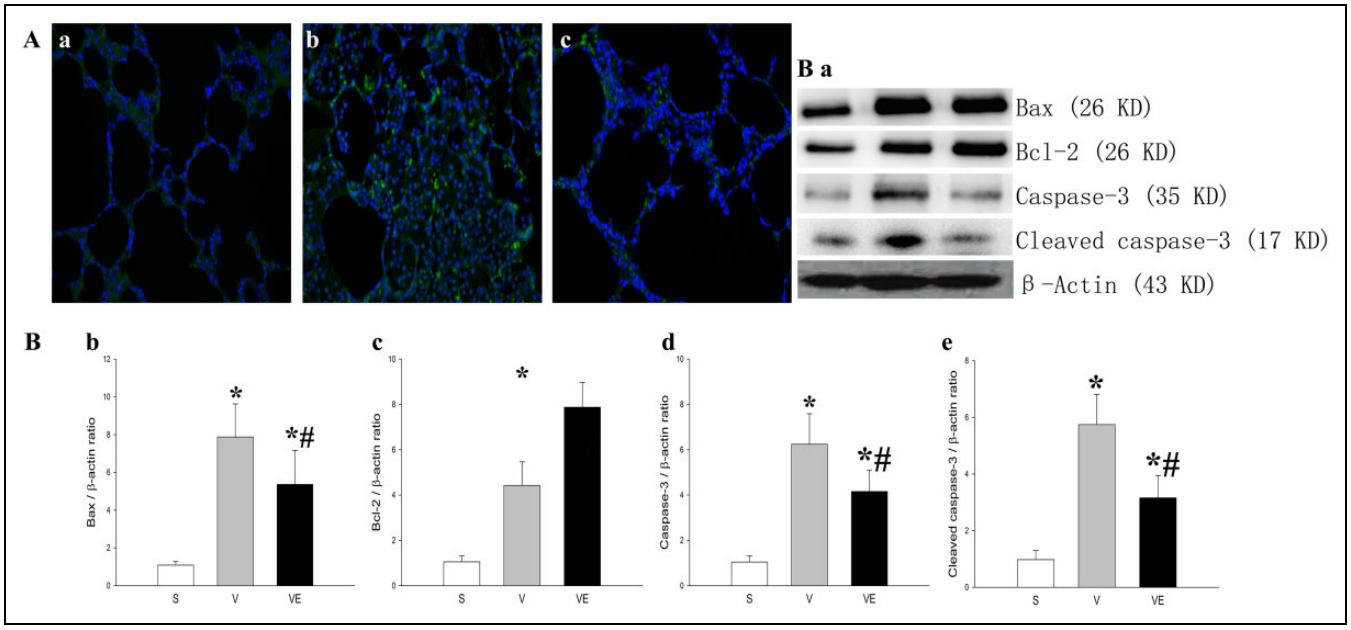

Figure 6. EPC transplantation mitigated the ventilation-induced apoptotic damage in lung tissue. The representative results of apoptosis in lung tissue in the S group (Aa), V group (Ab), and EPC transplantation (VE group; Ac) were detected by TUNEL staining using fluorescence microscopy (A, 400 × magnification). TUNEL-positive cells were stained green and the nucleus was stained blue with DAPI. The representative results of the protein expression of Bax (first panel of Ba and Bb), Bcl-2 (second panel of Ba and Bc), native caspase-3 (third panel of Ba and Bd), and cleaved caspase-3 (fourth panel of Ba and Be) in lung tissue in the S group (left bands of Ba, ☐), V group (middle bands of Ba; ☐) and VE group (right bands of Ba; ■) were detected by Western blot. The expression of the corresponding proteins was evaluated by densitometry analysis, and presented in Bb (Bax), Bc (Bcl-2), Bd (native caspase 3), and Be (cleaved caspase 3). Data in each group were calculated from three independent tests. $^{*}p < 0.05$ *vs.* the S group; $^{\#}p < 0.05$ *vs.* the V group. Abbreviations: EPCs, endothelial progenitor cells; S group, sham; TUNEL, terminal deoxynucleotidyl transferase dUTP nick end labeling; V group, VILI; VE group, VILI with EPC transplantation; VILI, ventilator-induced lung injury.

because the protection of EPCs on endothelial cells may due to the activation of NF-κB in the EPCs[48,49] themselves. Furthermore, the administration of inhibitors and agonists may influence the protective activity of EPCs.

In conclusion, the results in the present study indicate that EPC transplantation attenuates VILI. Furthermore, the pulmonary protective properties of EPCs might be attributed to the inhibition of MLC and NF-κB phosphorylation, and anti-

apoptotic activity through the downregulation of adhesion molecules and pro-inflammatory factors.

Ethics Approval

This study was approved by the Ethics Committee of Harbin Medical University.

Statement of Human and Animal Rights

All treatments were performed according to the Institutional Animal Care and Use Committee of the Second Affiliated Hospital of Harbin Medical University and national animal treatment guidelines.

Statement of Informed Consent

Since there were no human subjects in this manuscript, an informed consent was not required.

Declaration of Conflicting Interests

The author(s) declare no potential conflicts of interest with respect to the research, authorship, and/or publication of this manuscript.

Funding

The author(s) disclosed receipt of the following financial support for the research, authorship, and/or publication of this article: This research was supported by funds from the National Natural Science Fund (81500074) and Heilongjiang Natural Science Foundation (QC2017112 and YQ2019H009).

ORCID iD


Wei Gao https://orcid.org/0000-0001-5748-899X

References

1. Esteban A, Anzueto A, Alía I, Gordo F, Apezteguía C, Pálizas F, Cide D, Goldwaser R, Soto L, Bugedo G, Rodrigo C, et al. How is mechanical ventilation employed in the intensive care unit? An international utilization review. Am J Respir Crit Care Med. 2000;161(5):1450–1458.
2. Gajic O, Dara SI, Mendez JL, Adesanya AO, Festic E, Caples SM, Rana R, St Sauver JL, Lymp JF, Afessa B, Hubmayr RD. Ventilator-associated lung injury in patients without acute lung injury at the onset of mechanical ventilation. Crit Care Med. 2004;32(9):1817–1824.
3. Tobin MJ. Culmination of an era in research on the acute respiratory distress syndrome. N Engl J Med. 2000;342(18):1360–1361.
4. Caruso P. Ventilator-induced lung injury distribution: the key to understanding injury mechanisms. Am J Respir Crit Care Med. 2007;175(1):95–96; author reply 6.
5. Kneyber MC, Zhang H, Slutsky AS. Ventilator-induced lung injury. Similarity and differences between children and adults. Am J Respir Crit Care Med. 2014;190(3):258–265.
6. Brower RG, Matthay MA, Morris A, Schoenfeld D, Thompson BT, Wheeler A. Ventilation with lower tidal volumes as compared with traditional tidal volumes for acute lung injury and the acute respiratory distress syndrome. N Engl J Med. 2000;342(18):1301–1308.
7. Hager DN, Krishnan JA, Hayden DL, Brower RG. Tidal volume reduction in patients with acute lung injury when plateau pressures are not high. Am J Respir Crit Care Med. 2005;172(10):1241–1245.
8. Force ADT, Ranieri VM, Rubenfeld GD, Thompson BT, Ferguson ND, Caldwell E, Fan E, Camporota L, Slutsky AS. Acute respiratory distress syndrome: the Berlin Definition. JAMA. 2012;307:2526–2533.
9. Bellani G, Laffey JG, Pham T, Madotto F, Fan E, Brochard L, Esteban A, Gattinoni L, Bumbasirevic V, Piquilloud L, van Haren F, et al. Noninvasive ventilation of patients with acute respiratory distress syndrome. Insights from the LUNG SAFE Study. Am J Respir Crit Care Med. 2017;195(1):67–77.
10. Wilson MR, O'Dea KP, Zhang D, Shearman AD, van Rooijen N, Takata M. Role of lung-marginated monocytes in an in vivo mouse model of ventilator-induced lung injury. Am J Respir Crit Care Med. 2009;179(10):914–922.
11. Wilson MR, Choudhury S, Goddard ME, O'Dea KP, Nicholson AG, Takata M. High tidal volume upregulates intrapulmonary cytokines in an in vivo mouse model of ventilator-induced lung injury. J Appl Physiol (1985). 2003;95(4):1385–1393.
12. Hegeman MA, Hennus MP, Heijnen CJ, Specht PA, Lachmann B, Jansen NJ, van Vught AJ, Cobelens PM. Ventilator-induced endothelial activation and inflammation in the lung and distal organs. Crit Care. 2009;13(6):R182.
13. Verbrugge SJ, Lachmann B, Kesecioglu J. Lung protective ventilatory strategies in acute lung injury and acute respiratory distress syndrome: from experimental findings to clinical application. Clin Physiol Funct Imaging. 2007;27(2):67–90.
14. Kocher AA, Schuster MD, Szabolcs MJ, Takuma S, Burkhoff D, Wang J, Homma S, Edwards NM, Itescu S. Neovascularization of ischemic myocardium by human bone-marrow-derived angioblasts prevents cardiomyocyte apoptosis, reduces remodeling and improves cardiac function. Nat Med. 2001;7(4):430–436.
15. Mao M, Wang SN, Lv XJ, Wang Y, Xu JC. Intravenous delivery of bone marrow-derived endothelial progenitor cells improves survival and attenuates lipopolysaccharide-induced lung injury in rats. Shock. 2010;34(2):196–204.
16. Aggarwal S, Pittenger MF. Human mesenchymal stem cells modulate allogeneic immune cell responses. Blood. 2005;105(4):1815–1822.
17. Cao JP, He XY, Xu HT, Zou Z, Shi XY. Autologous transplantation of peripheral blood-derived circulating endothelial progenitor cells attenuates endotoxin-induced acute lung injury in rabbits by direct endothelial repair and indirect immunomodulation. Anesthesiology. 2012;116(6):1278–1287.
18. Siavashi V, Nassiri SM, Rahbarghazi R, Vafaei R, Sariri R. ECM-dependence of endothelial progenitor cell features. J Cell Biochem. 2016;117(8):1934–1946.
19. Gao X, Chen W, Liang Z, Chen L. Autotransplantation of circulating endothelial progenitor cells protects against lipopolysaccharide-induced acute lung injury in rabbit. Int Immunopharmacol. 2011;11(10):1584–1590.

20. Patschan D, Schwarze K, Tampe B, Zeisberg M, Patschan S, Muller GA. Endothelial Colony Forming Cells (ECFCs) in murine AKI - implications for future cell-based therapies. BMC Nephrol. 2017;18(1):53.
21. Muller HC, Witzenrath M, Tschernig T, Gutbier B, Hippenstiel S, Santel A, Suttorp N, Rosseau S. Adrenomedullin attenuates ventilator-induced lung injury in mice. Thorax. 2010;65(12): 1077–1084.
22. Gao W, Jiang T, Liu YH, Ding WG, Guo CC, Cui XG. Endothelial progenitor cells attenuate the lung ischemia/reperfusion injury following lung transplantation via the endothelial nitric oxide synthase pathway. J Thorac Cardiovasc Surg. 2019;157(2):803–814.
23. Kähler CM, Wechselberger J, Hilbe W, Gschwendtner A, Colleselli D, Niederegger H, Boneberg EM, Spizzo G, Wendel A, Gunsilius E, Patsch JR, et al. Peripheral infusion of rat bone marrow derived endothelial progenitor cells leads to homing in acute lung injury. Respir Res. 2007;8:50.
24. Ju YN, Yu KJ, Wang GN. Budesonide ameliorates lung injury induced by large volume ventilation. BMC Pulm Med. 2016; 16(1):90.
25. Gao W, Ju YN. Budesonide attenuates ventilator-induced lung injury in a rat model of inflammatory acute respiratory distress syndrome. Arch Med Res. 2016;47(4):275–284.
26. Farias LL, Faffe DS, Xisto DG, Santana MC, Lassance R, Prota LF, Amato MB, Morales MM, Zin WA, Rocco PR. Positive end-expiratory pressure prevents lung mechanical stress caused by recruitment/derecruitment. J Appl Physiol (1985). 2005;98(1):53–61.
27. Wrigge H, Zinserling J, Stuber F, von Spiegel T, Hering R, Wetegrove S, Hoeft A, Putensen C. Effects of mechanical ventilation on release of cytokines into systemic circulation in patients with normal pulmonary function. Anesthesiology. 2000;93(6):1413–1417.
28. Dudek SM, Garcia JG. Cytoskeletal regulation of pulmonary vascular permeability. J Appl Physiol (1985). 2001;91: 1487–1500.
29. Mirzapoiazova T, Moitra J, Moreno-Vinasco L, Sammani S, Turner JR, Chiang ET, Evenoski C, Wang T, Singleton PA, Huang Y, Lussier YA, et al. Non-muscle myosin light chain kinase isoform is a viable molecular target in acute inflammatory lung injury. Am J Respir Cell Mol Biol. 2011;44(1): 40–52.
30. Ma H, Feng X, Ding S. Hesperetin attenuates ventilator-induced acute lung injury through inhibition of NF-kappaB-mediated inflammation. Eur J Pharmacol. 2015;769:333–341.
31. Liu YY, Chiang CH, Chuang CH, Liu SL, Jheng YH, Ryu JH. Spillover of cytokines and reactive oxygen species in ventilator-induced lung injury associated with inflammation and apoptosis in distal organs. Respir Care. 2014;59(9): 1422–1432.
32. Owen CA, Hu Z, Barrick B, Shapiro SD. Inducible expression of tissue inhibitor of metalloproteinases-resistant matrix metalloproteinase-9 on the cell surface of neutrophils. Am J Respir Cell Mol Biol. 2003;29(3 Pt 1):283–294.
33. Miyao N, Suzuki Y, Takeshita K, Kudo H, Ishii M, Hiraoka R, Nishio K, Tamatani T, Sakamoto S, Suematsu M, Tsumura H, et al. Various adhesion molecules impair microvascular leukocyte kinetics in ventilator-induced lung injury. Am J Physiol Lung Cell Mol Physiol. 2006;290(6):L1059–L1068.
34. Kim JH, Suk MH, Yoon DW, Lee SH, Hur GY, Jung KH, Jeong HC, Lee SY, Lee SY, Suh IB, Shin C, et al. Inhibition of matrix metalloproteinase-9 prevents neutrophilic inflammation in ventilator-induced lung injury. Am J Physiol Lung Cell Mol Physiol. 2006;291(4):L580–L587.
35. Yu PJ, Li JR, Zhu ZG, Kong HY, Jin H, Zhang JY, Tian YX, Li ZH, Wu XY, Zhang JJ, Wu SG. Praeruptorin D and E attenuate lipopolysaccharide/hydrochloric acid induced acute lung injury in mice. Eur J Pharmacol. 2013;710:39–48.
36. Qiu J, Li W, Feng S, Wang M, He Z. Transplantation of bone marrow-derived endothelial progenitor cells attenuates cerebral ischemia and reperfusion injury by inhibiting neuronal apoptosis, oxidative stress and nuclear factor-kappaB expression. Int J Mol Med. 2013;31(1):91–98.
37. Wang Y, Fan L, Meng X, Jiang F, Chen Q, Zhang Z, Yan H. Transplantation of IL-10-transfected endothelial progenitor cells improves retinal vascular repair via suppressing inflammation in diabetic rats. Graefes Arch Clin Exp Ophthalmol. 2016;254(10):1957–1965.
38. Li S, Tian Y, Huang X, Zhang Y, Wang D, Wei H, Dong J, Jiang R, Zhang J. Intravenous transfusion of endothelial colony-forming cells attenuates vascular degeneration after cerebral aneurysm induction. Brain Res. 2014;1593:65–75.
39. Li LF, Liao SK, Ko YS, Lee CH, Quinn DA. Hyperoxia increases ventilator-induced lung injury via mitogen-activated protein kinases: a prospective, controlled animal experiment. Crit Care. 2007;11:R25.
40. Huang CS, Kawamura T, Lee S, Tochigi N, Shigemura N, Buchholz BM, Kloke JD, Billiar TR, Toyoda Y, Nakao A. Hydrogen inhalation ameliorates ventilator-induced lung injury. Crit Care. 2010;14(6):R234.
41. Cartron PF, Juin P, Oliver L, Meflah K, Vallette FM. Impact of proapoptotic proteins Bax and Bak in tumor progression and response to treatment. Expert Rev Anticancer Ther. 2003;3(4): 563–570.
42. Oikonomou N, Thanasopoulou A, Tzouvelekis A, Harokopos V, Paparountas T, Nikitopoulou I, Witke W, Karameris A, Kotanidou A, Bouros D, Aidinis V. Gelsolin expression is necessary for the development of modelled pulmonary inflammation and fibrosis. Thorax. 2009;64(6):467–475.
43. Christofidou-Solomidou M, Scherpereel A, Solomides CC, Muzykantov VR, Machtay M, Albelda SM, DiNubile MJ. Changes in plasma gelsolin concentration during acute oxidant lung injury in mice. Lung. 2002;180(2):91–104.
44. Lee PS, Waxman AB, Cotich KL, Chung SW, Perrella MA, Stossel TP. Plasma gelsolin is a marker and therapeutic agent in animal sepsis. Crit Care Med. 2007;35(3):849–855.
45. Messaris E. Actin-binding plasma gelsolin: a potential future ally in the fight against sepsis. Crit Care Med. 2007;35(3): 970–971.

46. Maniatis NA, Harokopos V, Thanassopoulou A, Oikonomou N, Mersinias V, Witke W, Orfanos SE, Armaganidis A, Roussos C, Kotanidou A, Aidinis V. A critical role for gelsolin in ventilator-induced lung injury. Am J Respir Cell Mol Biol. 2009;41(4):426–432.
47. Sieveking DP, Buckle A, Celermajer DS, Ng MK. Strikingly different angiogenic properties of endothelial progenitor cell subpopulations: insights from a novel human angiogenesis assay. J Am Coll Cardiol. 2008;51(6):660–668.
48. Mao SZ, Ye X, Liu G, Song D, Liu SF. Resident endothelial cells and endothelial progenitor cells restore endothelial barrier function after inflammatory lung injury. Arterioscler Thromb Vasc Biol. 2015;35(7):1635–1644.
49. Steinmetz M, Pelster B, Lucanus E, Arnal JF, Nickenig G, Werner N. Atorvastatin-induced increase in progenitor cell levels is rather caused by enhanced receptor activator of NF-kappaB ligand (RANKL) cell proliferation than by bone marrow mobilization. J Mol Cell Cardiol. 2013;57:32–42.